Malaysian Journal of Chemistry, 2024, Vol. 26(5), 112-124
(Special Issue: *3rd Virtual International Symposium on Sciences 2023*)

Highly Selective Removal of Ni(II) from Aqueous Solution using Crosslinked-Glutaraldehyde Chitosan Beads

Nurhani Lyana Ramli[1], Nur Sofiah Abu Kassim[1], Wan Nazihah Wan Ibrahim[2], Noor Hidayah Pungot[2] and Nurul Auni Zainal Abidin[1]*
[1]School of Chemistry and Environment, Faculty of Applied Sciences
Universiti Teknologi MARA (UiTM), Cawangan Negeri Sembilan, Kampus Kuala Pilah,
72000 Kuala Pilah, Negeri Sembilan, Malaysia
[2]Faculty of Applied Sciences, Universiti Teknologi MARA, 40450 Shah Alam, Selangor, Malaysia
*Corresponding author (e-mail: nurulauni@uitm.edu.my)

Heavy metals like nickel, chromium and copper have been excessively released into the environment due to rapid industrialization, which can cause a major global concern. There have been numerous studies done to remove heavy metals using various adsorbents such as chitosan. This study reports glutaraldehyde-crosslinked chitosan (GCC) beads as highly efficient bioadsorbents for the separation of nickel ions (Ni (II)) from aqueous solutions. With increasing the extent of glutaraldehyde-crosslinking, the GCC beads showed enhanced adsorption selectivity and capacity toward Ni (II). Fourier-transform infrared spectroscopy (FTIR) have been utilized for the characterization of the synthesized bioadsorbents. The effectiveness of GCC for Ni (II) removal in an aqueous solution at various parameters has been evaluated by flame atomic absorption spectroscopy (FAAS). The effects of parameters namely pH, agitation speed, contact time, adsorbent dose, and initial metal ion concentration were optimized by batch experiments. Under the optimum conditions, the adsorbent shows 91.97% for Ni (II) removal percent with good reusability till third cycle. Kinetic, isothermal, and thermodynamic analyses have been studied to have deep insights into the mechanism of Ni (II) on the synthesized adsorbents.

Keywords: Chitosan; crosslinked; nickel removal; adsorption; aqueous solution

Received: November 2023; Accepted: February 2024

Nickel (Ni) is one of the most common heavy metals released into the environment, cycled through the system via physical, chemical, and biological processes or transported by living things. Local industrial activities, such as plating, land-based disposal of sludges, solids, and slags, and disposal of effluents all contribute to the local anthropogenic nickel releases to the environment via water system. The burning of garbage and wood along with the combustion of fossil fuels are all examples of additional diffuse sources of nickel into the environment [1]. The excessive ingestion of nickel could lead to a series of adverse health impacts, such as respiratory problems, bone defects, nausea and vomiting, lung cancer and even neurological disorders such as depression and Alzheimer's disease [2]. According to the Water Pollutants Special Discharge Limit, the total Ni (II) standard assumes that Ni (II) concentration should be under 0.1 ppm [3]. Therefore, the demand for new natural-source materials to remove metal ions from industrial liquid waste is increasing. Researchers have investigated and implemented the application of renewable-based materials to remove such heavy metals.

In recent years, there have been countless articles on chitosan, with a focus on the applications and modification of these polymers. Chitosan is a linear polymer composed of glucosamine and N-acetylglucosamine sub-unit that are linked by β (1–4) linkages. Based on Figure 1, a huge number of function groups of hydroxyls (-OH) and amino group (-NH_2) can be observed in the polymer chain of chitosan. These function groups enhance chitosan's reactivity, causing it to easily react with a wide range of functional groups [4].

Chitosan is soluble in acidic media due to the protonation of free amino groups, and the precipitation tendency increases as the pH approaches 6.0, owing to the increase of NH_2 groups in the molecular structure. As a result of being insoluble in water, concentrated acids, acetone, and alcohol, amino groups allow them to bind to negatively charged materials such as other polysaccharides, enzymes, and cells [5]. It is also well recognised as a great biosorbent for heavy metal ion removal as it possesses several desirable properties including biodegradability, bioactivity, biocompatibility, and low toxicity. However, it also has critical flaws like low stability in acid, insufficient mechanical properties, low thermal stability, resistance to mass transfer, and low porosity and surface areas, resulting in a lower adsorption capacity for metal ion in aqueous solution [6]. To address these shortcomings, chitosan can undergo various modifications such as crosslinking and grafting, resulting in improved performance [4].

†Paper presented at the 3rd Virtual International Symposium on Sciences (3rd VISoS 2023)

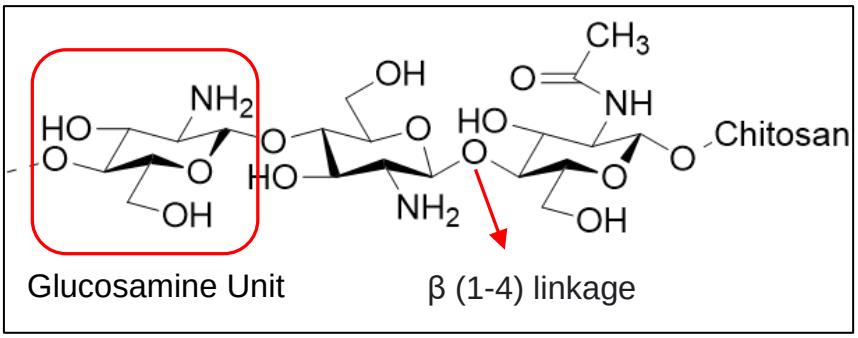

Figure 1. Chemical structure of chitosan

It was reported that the presence of reactive amino and hydroxyl groups in the structure of chitosan can cause it to be easily transformed into new modified forms [7]. There were several techniques that can be used in order to overcome these disadvantages which are by physical or chemical modification of chitosan. The modification of chitosan be carried out by physically which aimed to enhance its mechanical properties, reduce its crystallinity, and improve its swelling and diffusion properties. Meanwhile, it is also can be carried out by chemical method in order to improve its flexibility and chemical stability while decreasing its susceptibility in acidic environments [8].

Thus, this study aims to determine the effectiveness of modified chitosan for nickel ion removal in aqueous solution by using the adsorption method with the analysis of flame atomic absorption spectrometry (FAAS). The chitosan was modified by the crosslinking technique using glutaraldehyde crosslinker to inhibit the dissolution of chitosan when metal adsorption was conducted in acidic solution and to enhance the metal adsorption properties.

EXPERIMENTAL

Study Area

The Semenyih River in Selangor, Malaysia was chosen as the study location. It is located northeast of Hulu Langat, on the western slope of Banjaran Titiwangsa. The Semenyih River is a tributary of the Langat River that runs southward towards the districts of Hulu Langat and Sepang. This river has an average annual rainfall of about 3000 mm and is located between the longitudes 101°48'32.9" and 101°52'30.5" E and latitudes 2°54'14.9" and 03°03'23.1" N. The climate of this study area is defined by high humidity, a high average temperature, and uniform annual temperatures. Covering an area of 230.94 km^2, more than 1 million people today receive their drinking water from the Semenyih River. However, it has become increasingly contaminated due to agricultural activity effluent, direct discharge of untreated sewage, and industrial wastewater [9].

Figure 2. Map of the study area along the Semenyih River.

Table 1. List of Instruments.

Instruments	Makers	Function
Analytical balance	Sartorius (BT 224 S)	Weight Measurement
Hotplate	PRO Scientific (HPS-7A)	Consistent stirring
pH meter	Knick (765 Calimatic)	Measurement of pH
Fourier-transform infrared spectroscopy (FTIR)	Perkin Elmer (Spectrum 100)	Detection of functional groups
Flame atomic absorption spectrophotometer (FAAS)	Perkin Elmer (AAnalyst 700)	Estimation of metal ion concentration

Sampling Stations

Three sampling stations were selected along the river based on the characteristics of the water conditions. Figure 2 shows the sampling stations of the study area along the Semenyih River**.**

Station 1 (S1) is located subsequent to the town of Semenyih, where urban activities might have contributed to the river's pollution; Station 2 (S2) is located near industrial areas which may serve as the main source of heavy metal contamination; and Station 3 (S3) is located near residential areas affected by human activities. Three water samples were collected from each station. Water sampling was conducted during a sunny day by using a container attached to a long rope to ease collection. The grab sampling was carried out in the flowing river stream for not more than 15 minutes. Each water sample from each station was taken close to the left banks of the river. All samples were collected using 250 mL amber glass bottles. The samples were stored in a chiller at 4℃ prior to the analysis. The water samples were then filtered using a 0.45 µm nylon membrane filter (Whatman, Dassel, Germany). To eliminate the headspace, the bottles were filled to the rim. Subsequently, the samples were tested in the laboratory within 24 hours after collection on site.

Chemicals

The chemicals used in this experiment were 1M sodium hydroxide, 0.1 M of hydrochloric acid, 1% of aqueous acetic acid, and 1.7% of glutaraldehyde, chitosan powder and $NiSO_4$. All the chemicals were purchased from Sigma – Aldrich.

Apparatus

Mortar and pestle, beaker, Erlenmayer flask, funnel, filter paper, pH meter, petri dish, volumetric flask, measuring cylinder, magnetic stirrer, dropper, disposable syringe, sintered glass crucible, container, suction flask, retort stand, rubber filter adapter and centrifuge tube.

Instrumentation

The list of instruments used during the adsorption experiments along with their characterisation and functions is given in Table 1.

Method of Preparation of Crosslinked-Glutaraldehyde Chitosan Beads

The formation of crosslinked chitosan with glutaraldehyde was prepared by mixing 100 mL of 1 (%v/v) acetic acid solution into 2.5 g of chitosan powder, weighted by an analytical balance. The mixture was stirred constantly for 24 hours at room temperature using a magnetic stirrer. To enable the formation of chitosan beads with similar spherical size, the chitosan solution was introduced dropwise into 1M of sodium hydroxide solution using a disposable syringe. The formed beads were taken out of the solution after 24 hours and rinsed with distilled water until the pH value reached 7. Then, the chitosan beads were submerged for 12 hours in 25 mL of glutaraldehyde solution with a concentration of 1.7 (%v/v). Any unreacted particles were removed by washing the filtered crosslinked beads with distilled water and drying them in an oven at 60 °C for 10 hours [10].

Adsorption Experiment on River Water (Real Sample)

The adsorption experiment of nickel ions on the wastewater sample was performed in the following manner: 10 mL of wastewater sample was poured into a beaker. A pH value of 5.5 was obtained by dropping 0.1 M NaOH or 0.1 M HCl. Then, 0.3 g of glutaraldehyde-crosslinked chitosan was added to the beaker and stirred at 400 rpm. After 60 minutes of stirring, the sample was filtered using a filter funnel and analysed using flame atomic absorption spectroscopy to determine the concentration of nickel ion that remained.

Determination of Sorption Kinetic

The mechanism of the reaction and the reaction pathways are both essential insights provided by the kinetic analysis of adsorption in wastewater. Therefore, to obtain a good understanding of the adsorption mechanism and rate control steps, several kinetic models such as the pseudo-first-order kinetic model and pseudo-second-order kinetic model were proposed and used to analysed the experimental data [11].

Pseudo-First Order Model

The metal adsorption kinetics have frequently been predicted using the pseudo first-order kinetic model. The pseudo-first-order model estimates the rate of absorption, which is either proportional to the number of available vacant sites or not [4]. Other than that, it is also significant to show the physical adsorption that will take place on the adsorbent surface.

According to the pseudo-first-order model, the metal adsorption kinetics are given by:

$$\frac{dq}{dt} = k_1(q_e - q_t)$$

Where k_1 (min^{-1}) refers to the rate constant of the pseudo-first order adsorption, q_t is the amount of adsorption at time t (min) and q_e (mg/g) denotes the amount of adsorption at equilibrium.

Then, by using the constraints $q_t = 0$ at $t = 0$ and $q_t = q_t$ at $t = t$, gives

$$\log(q_e - q_t) = log q_e - \left(\frac{k_1}{2.303}\right) t$$

Therefore, the adsorption rate can be calculated by plotting $\log(q_e - q_t)$ versus t.

Pseudo-Second Order Model

Pseudo-second order model is also can be used further to examine the metal adsorption kinetic. This kinetic model estimates the rate is proportional to both the concentration of adsorbate and the number of unoccupied active sites. Additionally, it also demonstrates how electron transfer causes chemisorption to occur [4].

The equation for pseudo-second order model can be represented by:

$$\frac{dq}{dt} = k_2(q_e - q_t)^2$$

Then, by using the constraints qt = 0 at $t = 0$ and qt = qt at $t = t$, the latest equation will become:

$$\frac{t}{q_t} = \frac{1}{(k_2 q_e^2)} + \frac{t}{q_e}$$

k_2 (g/ (mg min)) defines as the rate constant, and from the intercept and slope, k_2 and q_e can be found.

Determination of Adsorption Isotherm

Adsorption isotherms are constructed by altering experimental parameters like the starting metal concentration and show how the adsorbate is distributed between the solid and liquid phases [12]. The most popular models for describing experimental data on adsorption are the Langmuir and Freundlich isotherms. These two isotherms were used in the current work to evaluate the adsorption of Ni(II) on crosslinked-glutaraldehyde beads under various conditions of process parameters. Metal concentrations ranging from 0.5 to 9.0 ppm were used in the adsorption equilibrium investigation.

Langmuir Isotherm Model

The Langmuir equation is one of the most basic models that may be used to explain equilibrium adsorption [13]. The Langmuir model assumes that the adsorption sites on the adsorbent have an equal affinity for the adsorbate, leading to the creation of an adsorbate monolayer [14]. The Langmuir equation can be observed as:

$$q_e = \frac{q_m K_L C_e}{1 + K_L C_e}$$

The linearization of the equation above will give the following form:

$$\frac{C_e}{q_e} = \frac{1}{q_m K_L} + \frac{C_e}{q_m}$$

Where C_e indicates equilibrium metal concentration, meanwhile the Langmuir constants that are corresponding to the maximum adsorption capacity (mg/g) and the relative energy of adsorption (l/mg) are q_m and K_L, respectively.

Freundlich Isotherm Model

Despite its simplicity compared to the others, Freundlich also is one the models that is most frequently used to determine the optimal isotherm fit. The Freundlich adsorption isotherm implies the different surface energy of adsorbent, the non-uniform of adsorption sites and the adsorption heat changes as the surface area is covered [15]. As a result, a typical heterogeneous surface's multilayer adsorption behaviour is described using the Freundlich model.

The Freundlich equation is represented by:

$$q_e = K_F C_e^{\frac{1}{n}}$$

The logarithmic of the equation above will give the following form:

$$\ln q_e = \ln K_F + \frac{1}{n} \ln C_e$$

The amount of metal ion adsorbed after adsorption per specific amount of adsorbent (mg/g) can be seen as q_e, meanwhile, the equilibrium concentration (mg/L) described as C_e and freundlich equilibrium is expressed by both K_F and n.

Removal Efficiency

The percentage of removal efficiency of metal ions can be generally explained as a percentage representing the number of metal ion removed or destroyed in comparison to the number of metal ion that entered the system. Therefore, the removal efficiency can be determined by the following equation:

$$R\% = \frac{(C_i - C_e)}{C_i} \times 100$$

Where R% is the percentage for metal ion removal meanwhile C_i and C_e is the initial and after batch experiment concentrations of metal ions, respectively [16].

RESULTS AND DISCUSSION

Fourier Transform Infrared Spectroscopy (FTIR)

This study successfully crosslinked chitosan with glutaraldehyde as a crosslinking agent. Figure 3 presents combination of FTIR spectra for raw chitosan (CH) and glutaraldehyde-crosslinked chitosan (GA-CH). The peaks in the range of 3200 to 3600 cm^{-1} can be attributed to O-H and N-H_2 bands stretching, both in chitosan and glutaraldehyde-crosslinked chitosan. Gierszewska who showed similar result stated that the addition of glutaraldehyde to chitosan has caused band stretching due to O-H and N-H_2 vibrations of chitosan functional groups engaged in hydrogen bonds to become wider [17].

Based on Figure 3(a), the absorption peaks at 3416 and 1646 cm^{-1} indicate the N-H stretching and bending of chitosan, respectively. In addition, the broad band observed at 3416 cm^{-1} indicates the O-H stretching vibration of the hydroxyl group. The peak at 2948 cm^{-1} is due to the C-H stretching of chitosan.

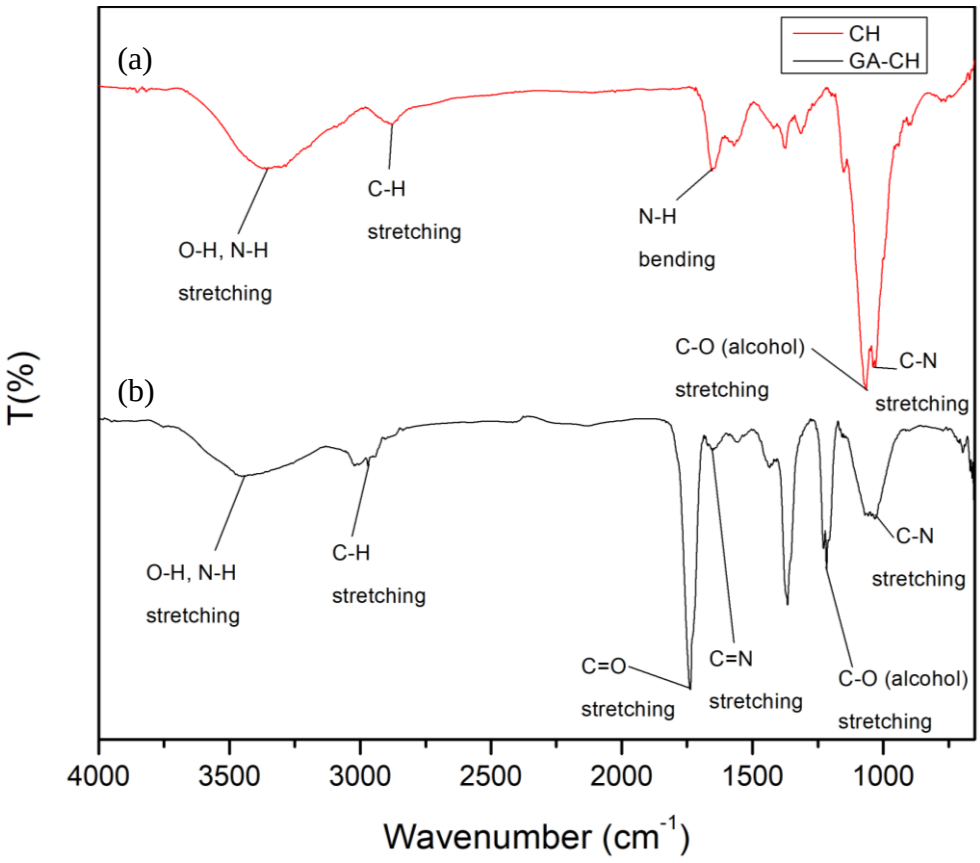

Figure 3. The FTIR spectra of (a) chitosan (CH) and (b) glutaraldehyde-crosslinked chitosan (GA-CH).

Table 2. The significant peaks of chitosan and glutaraldehyde-crosslinked chitosan.

Functional group	Chitosan (cm^{-1})	Glutaraldehyde-crosslinked chitosan (cm^{-1})
O-H, N-H stretching	3416, 3373	3458, 3448
C-H stretching	2948	2968
N-H bending	1645	-
C=N stretching	-	1653
C=O (aldehyde) stretching	-	1738
C-N stretching	1037	1033
C-O (alcohol) stretching	1065	1216

In addition, the peak at 1037 cm^{-1} corresponds to C-N stretching, and the broad band occurring around 1065 cm^{-1} was assigned to the primary alcohol C-O stretching as well as O-H bending vibrations. The spectra of glutaraldehyde-crosslinked chitosan (Figure 3(b)), the crosslinking process shifted the peak to 3448 cm^{-1}, suggesting that the hydrogen bonding between chitosan was interrupted by glutaraldehyde's presence. Furthermore, the peak at 1645 cm^{-1} was not present, while a sharp peak formed at 1653 cm^{-1} due to the formation of a Schiff base (imine linkage of C=N) between the aldehyde group in glutaraldehyde and the amino group in chitosan. Based on the spectra (Figure 3), the active sites that played a role in the formation of complexes with Ni (II) may be -N= and -OH. Bui *et al*. [18] stated that the differences between glutaraldehyde-crosslinked chitosan and the untreated chitosan in the size of the C-H vibration at 2968 cm^{-1} can be due solely to the increasing number of C-H bonds due to the increasing crosslinking chains of glutaraldehyde. Table 2 summarizes the functional groups that seen in the FTIR spectrum of chitosan and glutaraldehyde-crosslinked chitosan.

Effect of Adsorption Parameter

Effect of pH

According to Khiam *et al*. [19]**,** the pH of the solution has a significant impact on the adsorption of ions from aqueous solutions as it can modify the surface charge of the sorbent. Moreover, the solubility of metal ions in the solution and the degree of ionisation of the adsorbate during the adsorption process can also be influenced by the initial pH value [20]. Therefore, the effect of pH on the adsorption of Ni(II) was studied at three different pH values using glutaraldehyde-crosslinked chitosan beads. In order to study the effect of pH, the other parameters such as metal ion concentration (1 ppm), mass of adsorbent (0.1 g), agitation speed (200 rpm), contact time (120 min), and volume of metal ion solution used to immerse the adsorbent (10 mL) were kept constant.

The result indicates that the percentage of Ni(II) adsorption increased with the increase in pH until it reached pH 5.5. This is because of the protonation of the amino groups in the lower pH range had caused the adsorption capacity of the adsorbent to be weak at pH values lower than 5.0. Therefore, it will lower the number of binding sites available to Ni(II) for adsorption. Additionally, the protonation of amino groups caused the Ni(II) cations to repel one another electrostatically, thus resulting in poor adsorption efficiency. These findings are supported by Ibrahim *et al*. [20] who stated that at pH lower than 5.0, a positively charged surface is formed because the amino groups in the chitosan in glutaraldehyde-crosslinked chitosan beads are protonated in acidic solutions. Therefore, metal ion adsorption becomes quite challenging since electrostatic repulsion has occurred between the positively charged amino groups and the positive metal ions.

However, the protonated amino groups will lose the hydrogen ions and become deprotonated when the pH of the solution rises and the rivalry between the hydrogen ions and metal cations for adsorption is likewise lessened. This will increase the number of binding sites and the Ni(II) cations in the aqueous solution may interact with the active sites available for ion adsorption. According to Kayalvizhi *et al*. [21], if the pH of the aqueous solution is raised above 6.0, an incorrect interpretation of adsorption can occur since the precipitation of the ions as $Ni(OH)_2$ will take place. As a result, the maximum percentage adsorption of Ni(II) was about 7.59% at pH 5.5.

Effect of Agitation Speed

Adsorption studies of 0.1 g of adsorbent in a 10 ml solution at pH 5.5 for Ni(II) with an initial concentration of 1 ppm were performed at different agitation speeds between 60 and 600 rpm to observe its impact. The outcome values are illustrated in Figure 4. Adsorption was observed to increase with increasing agitation

speed. According to Kayalvizhi *et al*. [21], this is because when agitation speed increases, proper contact between the metal ion and the active site forms. Therefore, the diffusion of the metal ions to the adsorbent surface is accelerated by faster agitation. However, the adsorption capacity only significantly rises up to a certain point, which is when the stirring speed was 400 rpm and there was no observable increment of adsorption beyond the speed. Thus, the optimum agitation speed value is regarded as 400 rpm as it gave 56.44% of the adsorption of Ni(II).

Effect of Contact Time

One of the key components of a successful wastewater treatment system is the equilibrium time [22]. Thus, the impact of contact time on Ni(II) adsorption efficiency of 0.3 g glutaraldehyde-crosslinked chitosan beads was studied using a 10 mL solution at pH 5.5 with an initial concentration of 1 ppm. The adsorption studies were performed at different contact times between 30 and 150 min by stirring at 200 rpm to identify the equilibrium time.

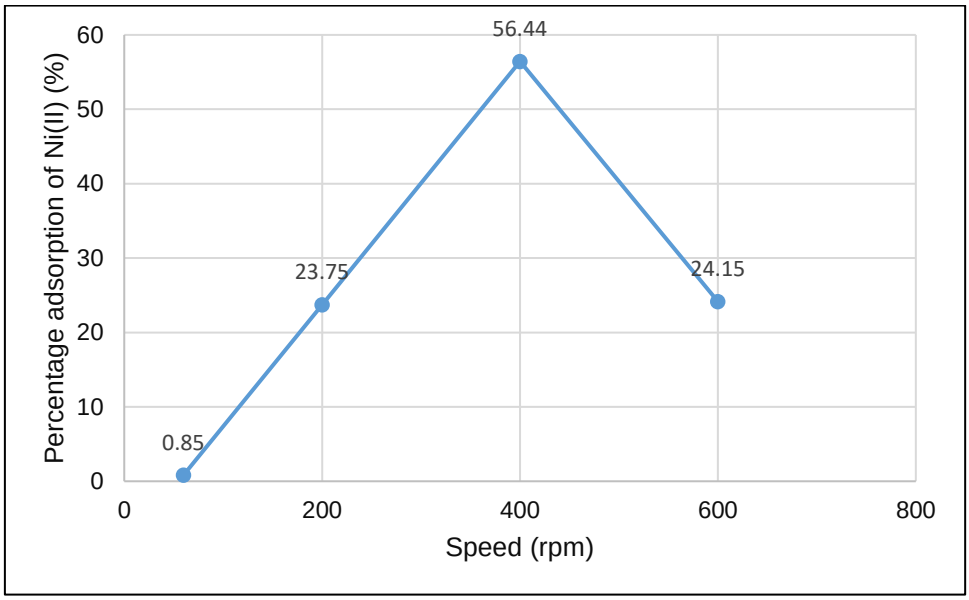

Figure 4. Effect of speed on the adsorption of Ni(II)

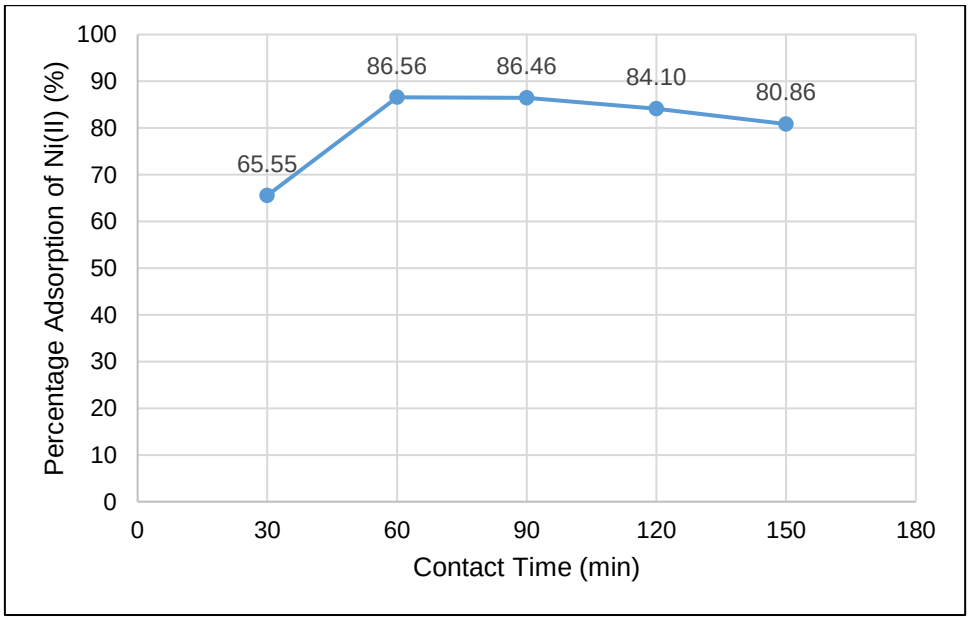

Figure 5. Effect of contact time on the adsorption of Ni(II)

Figure 5 reveals that the percentage removal of Ni(II) increased over time in the beginning of the stage (30 – 60 min), where it reached its highest percentage at 60 min with 87.53% percentage removal. According to Yadav *et al*. [23], it is possible that in the early stage of adsorption, there are more free adsorption binding sites present which causes the adsorption to rise at first. After all, as Ni(II) continues to bind to the binding sites, fewer binding sites are available for adsorption, resulting in a slower rate of adsorption. The empty sites on the surface became saturated as the adsorption process continues, and subsequently, the rate of adsorption plateaus at a constant value [21]. This can be observed in Figure 5, whereby as the contact time increased, the percentage adsorption of the metal ion decreased and became almost steady from 90 to 150 min. Therefore, the optimum contact time for the maximum adsorption of Ni(II) is 60 min.

Effect of Adsorbent Dose

According to Kuczajowska-Zadrożna *et al*. [24], the dose of a sorbent is also one of the parameters that strongly affect the sorption efficiency. Thus, the adsorption of 10 mL Ni(II) solution at a pH at 5.5 for was determined at four different doses of adsorbent ranging between 0.1 and 0.4 g for a fixed ion concentration of 1 ppm. The beads were stirred at 400 rpm for 60 minutes before being analysed on FAAS to determine the final concentration of Ni(II). Figure 6 shows that as the adsorbent dosage is increased, the adsorption percentage of the metal ion also rises. This improves the adsorbent removal effectiveness as it provides a higher number of active sites available for the adsorption of Ni(II) [19]. Figure 6 also depicts that when 0.3 g of glutaraldehyde-crosslinked chitosan beads was added into the aqueous solution, the percentage removal of Ni(II) reached the maximum as it absorbed about 89.31%. According to Nematidil *et al*. [25], as more time went by, saturation of the adsorption sites on the adsorbents' surfaces took hold since the equilibrium conditions had been achieved, preventing any more Ni(II) from adhering to them.

Effect of Initial Metal Ion Concentration

A total of 0.3 g glutaraldehyde-crosslinked chitosan beads were treated at different concentrations between 1 and 9 ppm with 10 mL solution of the Ni(II) ions at a solution pH of 5.5. The impact of initial metal ion concentration of Ni(II) adsorption capacity of the modified beads is depicted in Figure 7. The figure shows that the highest removal percentage of Ni(II) occurred when the initial metal concentration was 1 ppm at 89.31%, but it started to decrease when the initial metal ion concentration was increased to 3.0 ppm. This trend is similar to that observed by Kayalvizhi *et al*. [21] who found that the initial concentration of metal ions exists as a driving force to minimise the mass transfer from the adsorbent to the metal ions. This is because there are enough free active sites on the glutaraldehyde-crosslinked chitosan beads that are available to be occupied by metal ions at lower concentrations. However, as the concentration keeps on increasing, more metal ions remain unabsorbed due to the fixed number of free active sites. This will lower the adsorption of metal ions due to the increase in initial nickel concentration.

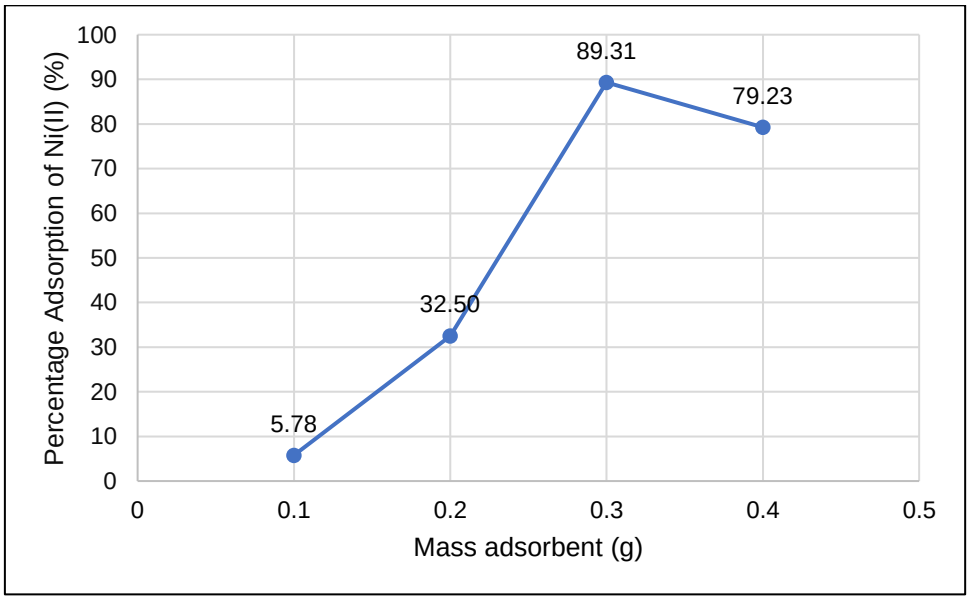

Figure 6. Effect of mass adsorbent on the adsorption of Ni(II)

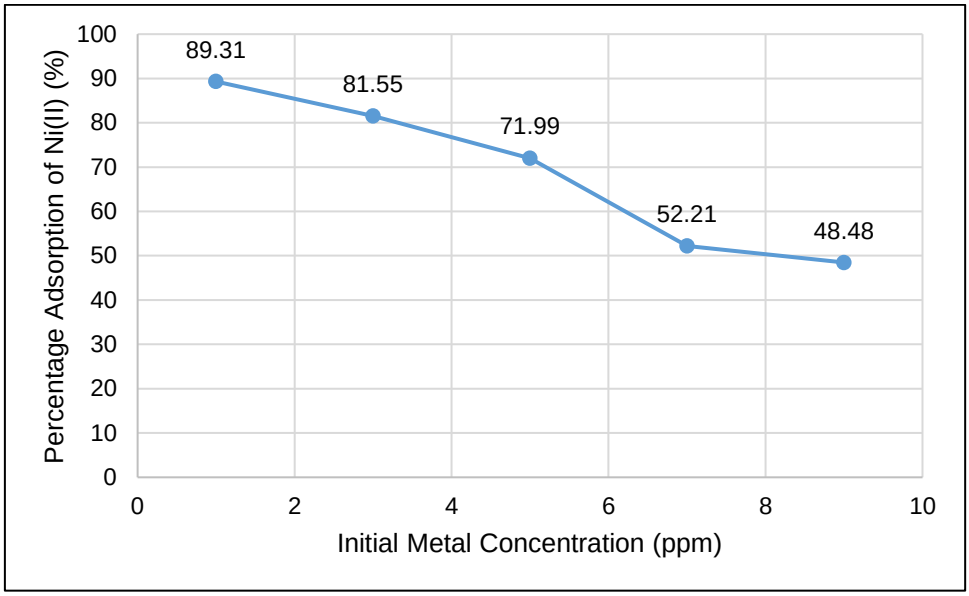

Figure 7. Effect of initial metal concentration on the adsorption of Ni(II)

Adsorption on River Water by Glutaraldehyde-crosslinked Chitosan

The experiment continued by treating the river water sample with glutaraldehyde-crosslinked chitosan beads. A sample of 10 mL river water was taken and analysed on FAAS to determine the initial concentration of Ni(II) in the sample; it was recorded to be 0.248 ppm. As a result, the optimum conditions obtained from previous experiments were used to calculate the percentage of Ni(II) adsorbed in the river water. Another 10 mL of river water was taken and adjusted to pH 5.5 before being treated with 0.3 g of glutaraldehyde-crosslinked chitosan beads. After 60 minutes of stirring at 400 rpm, the concentration of Ni(II) was reduced to 0.091 ppm, representing 63.31% of the adsorption percentage. It is shown that the adsorption percentage of Ni(II) is lower in wastewater compared to the aqueous solution (89.31%). As there are other metal cations in the wastewater, Zhao *et al.* [15] stated that this result is to be expected. Various metal cations such as K^+, Ca^{2+}, Na^+, and Mg^{2+} are often present in wastewater, which may interfere with the adsorption of Ni(II). It can also be stated that when interfering ions were present, the adsorption efficiency of Ni(II) was lower because they may have taken up residence at the active sites of the adsorbate and prevented the formation of bonds between the adsorbent and adsorbate [23]. Therefore, the presence of other metal cations in the sample will lead to competitive adsorption, which could affect the adsorption efficiency of heavy metal ions by the glutaraldehyde-crosslinked chitosan beads.

Sorption Kinetic

The widely used adsorption reaction kinetic models, pseudo-first and pseudo-second order models, are used in this kinetic study to understand the inherent kinetic mechanism involved in Ni(II) adsorption using glutaraldehyde-crosslinked chitosan beads. The graph of pseudo-first and pseudo-second order models are depicted in Figure 8 and Figure 9, respectively. The correlation coefficient (R^2) is evaluated for all the investigated kinetic models using liner approaches because it is the metric that is most frequently used to choose the best kinetic model. The kinetics of adsorption was studied for a contact time ranging from 30 to 150 min. Based on the graph, it can be observed that the pseudo-second kinetic order provided a R^2 value of 0.9894, indicating that this model better explains the Ni(II) adsorption process. On the other hand, the R^2 value in the pseudo-first order model is lower than in the pseudo-second order model. As a result of the low correlation coefficient, this model was deemed unsuitable for describing the kinetic behaviour of Ni(II) adsorption onto the glutaraldehyde-crosslinked chitosan adsorbent. Hence, this adsorption system seems to follow the pseudo-second order kinetic model.

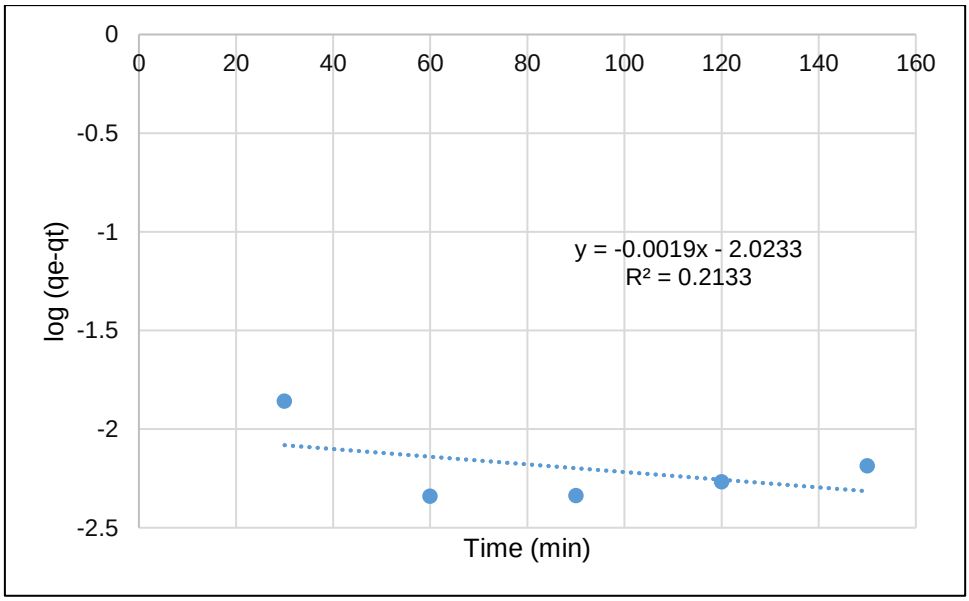

Figure 8. Pseudo-first order kinetic plot for Ni(II) adsorption.

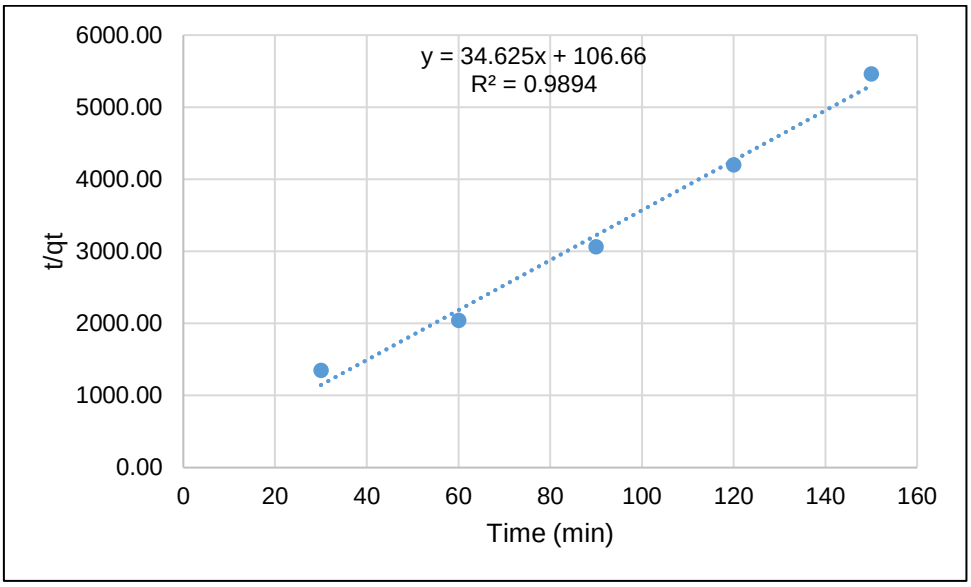

Figure 9. Pseudo-second order kinetic plot for Ni(II) adsorption.

Sorption Isotherm

Adsorption isotherm is usually described as the relationship between the adsorption concentration and the degree of adsorption. According to Mallik *et al.* [26], they stated that to maximise the utilisation of adsorbents, isotherm studies are essential to understand on how the active sites of the adsorbents are distributed. Moreover, the isotherm also reveals information about the adsorbent's maximum sorption capacity. In this study, the equilibrium properties of the adsorption of Ni(II) by glutaraldehyde-crosslinked chitosan have been addressed by using the classical adsorption isotherms which are Langmuir and Freundlich isotherms. These isotherm models are the most frequent example of isotherms used to explain the adsorption of heavy metal ions on the adsorbent surface. According to Kayalvizhi *et al.* [21], when metal ions are adsorbed on a homogenous adsorbent surface with monolayer coverage, the Langmuir isotherm model is the one that best fits experimental data. The Freundlich isotherm model, on the other hand, is applicable when metal ion multilayer adsorption takes place on a heterogeneous adsorbent surface [27].

Table 3. Isotherm constants for Ni(II).

Isotherms	Values
Langmuir	
q_m (mg/g)	0.3609
K_L (L/mg)	0.4245
R_L	0.6737
R^2	0.9957
Freundlich	
K_F (mg/Kg)	0.0039
n	2.6089
R^2	0.9118

The relevant data employed for the study of these isotherms are compiled in Table 3. The Langmuir isotherm model showed the best fitting with a correlation coefficient (R^2) value of 0.9957 of experimental data compared to Freundlich (R^2 = 0.9118). In this case, the correlation coefficient is close to 1, and the values for error function are low. Furthermore, the isotherm studies also informed us the maximum adsorption capacity of the adsorbent. The maximum adsorption capacity for Ni(II) adsorption onto the glutaraldehyde-crosslinked chitosan of 0.3609 mg g^{-1} was obtained. Unfortunately, the maximum adsorption capacity for Ni(II) adsorption onto the raw chitosan could not be obtained since the experiment was not performed. However, Popa *et al*. [28] stated that modification of chitosan gave the adsorbent a higher active site and higher specific surface area which led to the development of a higher adsorption capacity from 21 mg g^{-1} to 50.25 mg g^{-1}.

As for the separation factor (R_L) value, it is calculated to be 0.674 which are less than one and higher than zero. The positive adsorption of Ni(II) onto glutaraldehyde-crosslinked chitosan appears to be a favourable process since the value of R_L is lies within the range of 0 to 1 [29]. As for Freundlich, the constant K_F will stands for the sorbent's sorption capacity meanwhile the 'n' value is calculated to be 2.61. This value represents a favourable adsorption since the 'n' value lies between 1 and 10.

CONCLUSION

In this study, glutaraldehyde-crosslinked chitosan beads were successfully modified for the removal of nickel ions. The chemical modification of chitosan has been accomplished by using a crosslinker, glutaraldehyde. The crosslinked chitosan has also been modified physically to mould chitosan powder into a different morphology, which is spherical beads. The adsorbent has shown promising results in removing nickel ions from the aqueous solution and wastewater. Adsorption kinetic studies revealed that the adsorption of Ni(II) by glutaraldehyde-crosslinked chitosan followed a pseudo-second order kinetic model since it provided the best correlation with the experimental data (R^2 = 0.9894). The adsorption data were then fitted to different isotherm models, and the Langmuir model was found to be the best one with an R^2 value of 0.9957. This adsorption isotherm investigation also confirmed that the maximum adsorption capacity of Ni(II) by glutaraldehyde-crosslinked chitosan was 0.3609 mg/g.

ACKNOWLEDGEMENTS

The authors would like to acknowledge the Faculty of Applied Sciences, Universiti Teknologi Mara (UiTM), Cawangan Negeri Sembilan, Kampus Kuala Pilah Campus for facilities and services provided for the analysis.

REFERENCES

1. Buxton, S., Garman, E., Heim, K. E., Lyons-Darden, T., Schlekat, C. E., Taylor, M. D., & Oller, A. R. (2019). Concise review of nickel human health toxicology and ecotoxicology. *Inorganics*, **7(7)**, 1–38.

2. Hatzikioseyian, A., Saikia, S., & Lens, P. N. L. (2022). Nickel removal by biogenic selenium nanoparticles (SeNPs): Characterization and simulation of non-symmetric breakthrough curves in continuous-flow packed-bed columns. *Environmental Nanotechnology, Monitoring and Management*, **18**, 1–18.

3. Costa, J. M., Costa, J. G. dos R. da & Almeida Neto, A. F. de. (2022) Techniques of nickel(II) removal from electroplating industry wastewater: Overview and trends. In *Journal of Water Process Engineering, Elsevier Ltd.*, **46**, 1–14.

4. Sheth, Y., Dharaskar, S., Khalid, M., & Sonawane, S. (2021). An environment friendly approach for heavy metal removal from industrial wastewater using chitosan based biosorbent: A review. *Sustainable Energy Technologies and Assessments*, **43**, 1–29.

5. Santos, V. P., Marques, N. S. S., Maia, P. C. S. V., de Lima, M. A. B., Franco, L. de O. & de Campos-Takaki, G. M. (2020) Seafood waste as attractive source of chitin and chitosan production and their applications. *International Journal of Molecular Sciences*, **21(12)**, 1–17.

6. Vakili, M., Deng, S., Li, T., Wang, W., Wang, W., & Yu, G. (2018). Novel crosslinked chitosan for enhanced adsorption of hexavalent chromium in acidic solution. *Chemical Engineering Journal*, **347**, 782–790.

7. Parlayici, Ş. & Pehlivan, E. (2021) Modified Chitosan Forms for Cr (VI) Removal. *www.intechopen.com*

8. Al-Rooqi, M. M., Hassan, M. M., Moussa, Z., Obaid, R. J., Suman, N. H., Wagner, M. H., Natto, S. S. A. & Ahmed, S. A. (2022) Advancement of chitin and chitosan as promising biomaterials. *Journal of Saudi Chemical Society*, **26(6)**, 1–12.

9. Kasmuri, N., Mohamad, N. F. S., Jamil, S. S. M., Ahmad, R., Santiagoo, R., & Ramasamy, S. (2021) Assessment of water quality and heavy metals in Semenyih River. *IOP Conference Series: Earth and Environmental Science*, **646(1)**.

10. Galan, J., Trilleras, J., Zapata, P. A., Arana, V. A., & Grande-Tovar, C. D. (2021). Optimization of chitosan glutaraldehyde-crosslinked beads for reactive blue 4 anionic dye removal using a surface response methodology. *Life*, **11(2)**, 1–20.

11. Yang, Y., Zeng, L., Lin, Z., Jiang, H., & Zhang, A. (2021). Adsorption of Pb^{2+}, Cu^{2+} and Cd^{2+} by sulfhydryl modified chitosan beads. *Carbohydrate Polymers*, **274**, 1–9.

12. Pal, P., & Pal, A. (2019). Treatment of real wastewater: Kinetic and thermodynamic aspects of cadmium adsorption onto surfactant-modified chitosan beads. *International Journal of Biological Macromolecules*, **131**, 1092–1100.

13. Pires, A. B., Vitali, L., Tavares, A., Germano, C. A., Amorim, S. M., Moreira, R. F. P. M., Peralta, R. A., & Neves, A. (2021). Chitosan functionalized with heptadentate dinucleating ligand applied to removal of nickel, copper and zinc. *Carbohydrate Polymers*, **256**, 1–8.

14. Li, Y., Dong, X., & Zhao, L. (2021) Application of magnetic chitosan nanocomposites modified by graphene oxide and polyethyleneimine for removal of toxic heavy metals and dyes from water. *International Journal of Biological Macromolecules*, **192**, 125.

15. Zhao, N., Huang, H., Lv, X., Li, J., Guo, G. & Liu, Y. (2020) Removal of Cr(III) from aqueous solutions using waste kelp-derived biochar. *Desalination and Water Treatment*, **188**, 223–231.

16. Rahaman, M. H., Islam, M. A., Islam, M. M., Rahman, M. A., & Alam, S. M. N. (2021). Biodegradable composite adsorbent of modified cellulose and chitosan to remove heavy metal ions from aqueous solution. *Current Research in Green and Sustainable Chemistry*, **4**, 1–8.

17. Gierszewska, M., Jakubowska, E. & Olewnik-Kruszkowska, E. (2019) Effect of chemical cross-linking on properties of chitosan-montmorillonite composites. *Polymer Testing*, **77**, 1–11.

18. Bui, T. H., Lee, W., Jeon, S. B., Kim, K. W. & Lee, Y. (2020) Enhanced Gold(III) adsorption using glutaraldehyde-crosslinked chitosan beads: Effect of crosslinking degree on adsorption selectivity, capacity, and mechanism. *Separation and Purification Technology*, **248**, 1–12.

19. Khiam, G. K., Karri, R. R., Mubarak, N. M., Khalid, M., Walvekar, R., Abdullah, E. C., & Rahman, M. E. (2022). Modelling and optimization for methylene blue adsorption using graphene oxide/chitosan composites via artificial neural network-particle swarm optimization. *Materials Today Chemistry*, **24**, 1–14.

20. Ibrahim, A. G., Saleh, A. S., Elsharma, E. M., Metwally, E. & Siyam, T. (2019) Chitosan-g-maleic acid for effective removal of copper and nickel ions from their solutions. *International Journal of Biological Macromolecules*, **121**, 1287–1294.

21. Kayalvizhi, K., Alhaji, N. M. I., Saravanakkumar, D., Mohamed, S. B., Kaviyarasu, K., Ayeshamariam, A., Al-Mohaimeed, A. M., AbdelGawwad, M. R. & Elshikh, M. S. (2022) Adsorption of copper and nickel by using sawdust chitosan nanocomposite beads – A kinetic and thermodynamic study. *Environmental Research*, **203**, 1–8.

22. Rosli, N., Yahya, W. Z. N. & Wirzal, M. D. H. (2022) Crosslinked chitosan/poly(vinyl alcohol) nanofibers functionalized by ionic liquid for heavy metal ions removal. *International Journal of Biological Macromolecules*, **195**, 132–141.

23. Yadav, S., Asthana, A., Singh, A. K., Patel, J., Sreevidya, S., & Carabineiro, S. A. C. (2022). Facile preparation of methionine-functionalized graphene oxide/chitosan polymer nanocomposite aerogel for the efficient removal of dyes and metal ions from aqueous solutions. *Environmental Nanotechnology, Monitoring and Management*, **18**, 1–16.

24. Kuczajowska-Zadrożna, M., Filipkowska, U. & Jóźwiak, T. (2020) Adsorption of Cu (II) and Cd

(II) from aqueous solutions by chitosan immobilized in alginate beads. *Journal of Environmental Chemical Engineering*, **8(4)**, 1–7.

25. Nematidil, N., Sadeghi, M., Nezami, S. & Sadeghi, H. (2019) Synthesis and characterization of Schiff-base based chitosan-g-glutaraldehyde/ NaMMTNPs-APTES for removal Pb^{2+} and Hg^{2+} ions. *Carbohydrate Polymers*, **222**, 1–13.

26. Mallik, A. K., Kabir, S. F., bin Abdur Rahman, F., Sakib, M. N., Efty, S. S. & Rahman, M. M. (2022) Cu(II) removal from wastewater using chitosan-based adsorbents: A review. *Journal of Environmental Chemical Engineering*, **10(4)**, 1–22.

27. Abidin, N. A. Z., Kassim, N. S. A. K., Izzadin, S. A., Ghazali, S. M., Pungot, N. H. & Kamni, S. S. (2021) Evaluation of Heavy Metals Concentration in Milk Products by using Atomic Absorption Spectroscopy. *EKSAKTA: Journal of Sciences and Data Analysis*, **2(2)**, 136–141.

28. Popa, A., Visa, A., Maranescu, B., Hulka, I. & Lupa, L. (2021) Chemical modification of chitosan for removal of Pb(II) ions from aqueous solutions. *Materials*, **14(24)**, 1–18.

29. Rahangdale, D. & Kumar, A. (2018) Acrylamide grafted chitosan based ion imprinted polymer for the recovery of cadmium from nickel-cadmium battery waste. *Journal of Environmental Chemical Engineering*, **6(2)**, 1–12.